

# Photonic Crystal Fiber Array for True-Time-Delay Structured X-band Phased Array Antenna Systems

Yongqiang Jiang <sup>a,\*</sup>, Tao Ling <sup>a</sup>, Maggie Y. Chen <sup>b</sup>, Ray T. Chen <sup>a</sup>  
*a) Microelectronic Research Center, the University of Texas at Austin, Austin, TX 78758, USA*  
*b) Omega Optics, Austin, TX 78758, USA*  
*\*Author email address: yqjiang@ece.utexas.edu*

**ABSTRACT:** Tunable optical true-time-delay modules based on highly dispersive photonic crystal fibers were demonstrated to provide continuous radio frequency squint-free beam scanning for X-band phased array antenna systems.

© 2006 Optical Society of America

**OCIS codes:** (060.2310) Fiber Optics; (280.5110) Phased-Array Radar

## 1. Introduction

Phased-array antennas (PAAs) have the advantages of high directivity and quick beam steering without physical movement. Each antenna element of a PAA must have the correct phase condition to accomplish the desired beam scanning. However, the conventional electrical phase trimmer technique is intrinsically narrow-band and introduces beam squint. Recently, there has been growing interest in optical true time delay (TTD) techniques with the features of wide bandwidth, compact size, reduced system weight, and low electromagnetic interference when compared with electrical TTD techniques [1-2]. However, most of the optical TTD techniques require a large number of precisely time-delay matched optical elements such as lasers and optical delay segments resulting in a complex system design. Esman et al proposed a fiber-optic TTD technique using conventional dispersion compensating fiber (DCF) to meet these requirements [2]. However, its dispersion parameter  $D$ , of conventional DCF is of fairly small magnitude ( $D = -100$  ps/nm·km), and therefore long lengths of it are still needed in the TTD module to get the required delay. If the fiber group velocity dispersion is increased, the total fiber length will be decreased proportionally.

Conventional single-mode fibers (SMFs), based on weakly guiding structures of doped silica, can be tailored slightly to increase the dispersion by increasing the refractive index difference between the core and cladding [3]. However, dispersion cannot be changed significantly because of the small index variation across the transverse cross section from doping. This shortcoming can be overcome by the employment of high dispersion photonic crystal fibers (PCFs). PCFs have generated a lot of interest due to their unusual and attractive properties [3-7]. They are usually made of silica or polymer material with a regular hexagonal array of sub-micrometer-sized air holes running along the fiber as a cladding. A defect, usually one or multiple missing holes, acts as core. The dispersion of the PCFs is tuned by changing the pitch ( $\Lambda$ ) of the periodic array, the hole diameter ( $d$ ) and the doping concentration ( $n$ ) of the core, as shown in Fig. 1. [3-5]

In this summary, we implement a novel optical TTD module using an array of highly dispersive PCF. The TTD module is designed, fabricated and evaluated. The approach is based on highly dispersive PCF reported herein and other commercially available components and has potentially high reliability and stability as it requires no physically moving parts and no critical optical alignments. This is the first system demonstration to employ PCF based TTD modules for control of an X-band PAA system. The RF phase as the function of RF frequency is measured to verify that the time delay is independent of RF frequency. The wide instantaneous bandwidth of the TTD module is confirmed by measurements of the far-field patterns of the X-band PAA at two X-band frequencies.

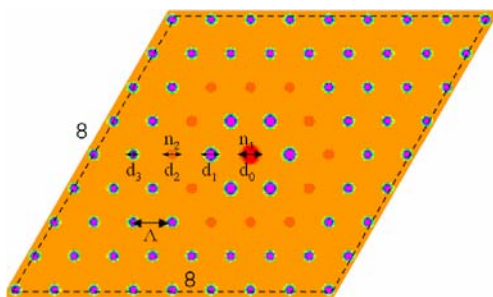


Fig.1. Transverse section of a model highly dispersive PCF. The box with dimensions  $D \times D$  corresponds to the supercell used to implement boundary conditions.

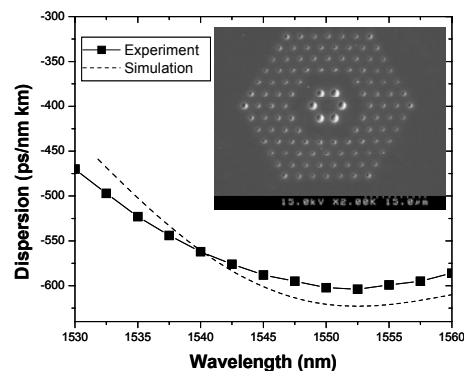


Fig. 2. The simulated and measured chromatic dispersion parameter  $D$  for highly dispersive PCFs. Insert is a scanning electron micrograph (SEM) image of the fabricated highly dispersive PCF.

## 2. True-time-delay module design, fabrication and characterization

We use a two-core PCF design to achieve high dispersion. The inner core is a doped silica rod instead of a missing hole, and the outer core is 12 concentric doped silica rods instead of missing holes, as shown in Fig. 1. Both cores are doped to have higher refractive index than pure silica, but the refractive index of the inner core is greater than that of the outer core. This two-core PCF can support two supermodes, which are analogous to the two supermodes of a directional coupler [6]. These modes are nearly phase matched at 1550 nm. Close to the phase matching wavelength, the mode index of the PCF changes rapidly due to strong coupling between the two individual modes of the inner core and outer core. Due to strong refractive index asymmetry between the two cores, there is a rapid change in the slope of the wavelength variation of the fundamental mode index. This leads to a large dispersion around 1550 nm. The air hole structure helps not only to guide the mode, but also to increase the dispersion value [6].

The dispersion of PCFs can be calculated using the full vectorial plane-wave expansion (PWE) method, which is fast and accurate compared to other methods [7]. Since our PCF design is not a perfect crystal without defects, we need to use a supercell having a size of  $N \times N$  instead of a natural unit cell to implement the periodic boundary conditions [7]. As shown in Fig. 1 an  $8 \times 8$  supercell is used for simulation purposes. Here  $8 \times 8$  meets the simulation convergence compared with  $7 \times 7$  and  $9 \times 9$ .

The dispersion parameter,  $D(\lambda)$ , of PCF is strongly related to the structure and refractive index perturbation, and can thus be changed to achieve the desired characteristics [3-5]. In our design, we use different doping concentrations,  $\Lambda$ ,  $d_0$ ,  $d_1$ ,  $d_2$ ,  $d_3$ , as shown in Fig. 1, to tune the dispersion. Here  $d_0$  and  $d_2$  are the diameters of the inner and outer doped silica rods, respectively. And  $d_1$  and  $d_3$  are the diameters of the air holes. Fig. 2 shows the theoretical simulation results of highly dispersive PCFs using the PWE method. The highest dispersion about  $-630$  ps/nm·km is obtained at 1552.5 nm. The highly dispersive PCF is fabricated using the stack-and-draw technique, where silica glass capillaries are stacked in a desired lattice array, fused together, and then drawn down to PCF. [4]. The scanning electron micrograph (SEM) image of the cross section is shown in the insert of Fig. 2. In order to measure the chromatic dispersion of the fabricated highly dispersive PCFs, we measured the time delay between optical wavelengths of  $\lambda_0 \pm 0.1$  nm. To obtain the time delay, we measured the phase difference between optical wavelengths ( $\lambda_0 + 0.1$  nm) and ( $\lambda_0 - 0.1$  nm) that are modulated at different microwave frequencies. The time delay can be derived from the slope of the each curve. The fiber chromatic dispersion is defined as  $\Delta T / (\Delta \lambda \cdot L)$  which can be obtained from the time delay divided by fiber length and laser wavelength difference 0.2 nm. The dispersion is  $-600$  ps/nm·km at 1550 nm, as shown in Fig. 2. The dispersion is increased by 33 times compared to telecom SMF-28 which has a dispersion parameter of 18 ps/nm·km, and by 6 times compared to conventional DCF.

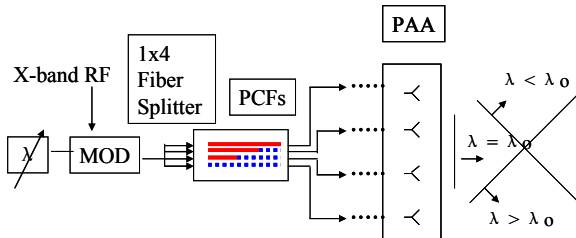


Fig. 3. Highly dispersive PCF enhanced wavelength continuous tunable PAA system structure. (Dashed line: highly dispersive PCF; solid line: Lucent TrueWave SMF; MOD: modulator)

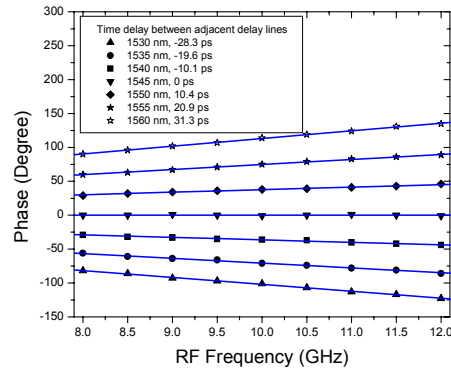


Fig. 4. Measured phase as a function of frequency. The time delays between two adjacent delay lines are calculated from the slope of the phase versus RF frequency.

A  $1 \times 4$  TTD module is designed and assembled using the fabricated highly dispersive PCF delay lines mentioned above. The lengths of the highly dispersive PCFs are 10.5m, 7.0m, 3.5m and 0m, as shown in Fig. 3. The measured insertion losses of the delay lines are 3.4 dB, 3.3 dB, 3.2 dB, 0.5 dB, respectively. Each delay line has the same nominal group delay at the central tuning wavelength 1545 nm but with slightly different net dispersion. This can easily be constructed by connecting varying lengths of highly dispersive PCFs and Lucent TrueWave SMF ( $D \approx 3$  ps/nm·km from 1530nm to 1565nm). The relative delay of the signals among the delay lines can thus be changed by tuning the optical wavelength. At the central tuning wavelength  $\lambda_0$ , 1545 nm, all the time delays are matched by trimming the TrueWave SMF. Thus, at  $\lambda_0$  the main antenna beam will be directed broadside. At wavelengths deviating from  $\lambda_0$ , each of the fiber delay lines generates a time delay proportional to its dispersion parameter,  $D$ , and the highly dispersive PCF length, resulting in a phase change to steer the main antenna radiation beam. [2]

The measured phase difference versus modulation frequency curves at different wavelengths are shown in Fig. 4. The time delay shown in the inset is derived from the slope of each curve. The wavelength at 1545 nm was chosen as a reference for zero time delay. By tuning the wavelength from 1528 nm to 1560 nm, different time delays can be achieved ranging from  $-31$  ps to 31

ps between any two adjacent delay lines. This is equivalent to scanning angles ranging from  $-45^\circ$  to  $45^\circ$  for a 2-bit 4-element PAA subarray having half-wavelength spacing at 10GHz. The linearity of phase versus frequency curve verifies the true-time delay and wide bandwidth capability of the proposed scheme.

### 3. System measurement

The assembled 4-element X-band PAA system is demonstrated and the block diagram is shown in Fig. 3. A microwave signal is generated from the HP network analyzer [8]. The optical carrier from the tunable laser (tuning range: 1520-1580nm, spectral width: 200MHz, tuning resolution:  $<0.024\text{nm}$ ) is distributed into the four sub-units of the TTD delay lines by a one-to-four fiber splitter. After the pre-determined time delay, the optical signals with correct phase relationships are detected by InGaAs high-speed photodetectors and individually fed into four antenna elements after amplification.

The far field pattern of the PAA is measured to verify the instantaneous RF broadband characteristics at frequencies of 9 GHz and 10.3 GHz. Fig. 5 shows the far field patterns at  $23^\circ$  scanning angle corresponding to a 17 ps delay time using a laser wavelength of 1553 nm (compared to the reference wavelength of 1545 nm that results in  $0^\circ$  scanning). From Fig. 5, it can be seen that the simulation results and measured data agree fairly well. The deviation from the theoretical prediction shown in Fig. 5 is due to the non-uniformity of the 4 radiation elements. As expected, the measurement shows no beam squint effect.

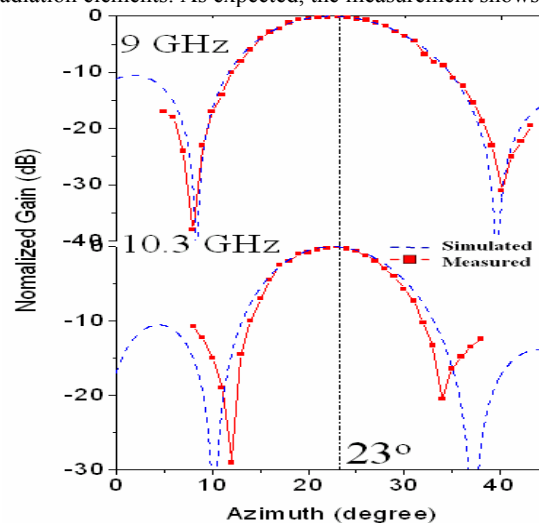


Fig. 5. Comparison of far-field patterns of the PAA at  $23^\circ$  scanning angle at frequencies of 9 and 10.3 GHz with an optical wavelength of 1553 nm.

### 4. Acknowledgments

The X-band testbed of the antenna system was supported by Air Force Office of Scientific Research (AFOSR) and by the Missile Defense Agency (MDA). The X-band phased array antenna array was provided by the Air Force Research Laboratory (AFRL). The photonic crystal fiber work reported herein for the true time delay application is currently supported by the Defense Advanced Research Project Agency (DARPA).

### 5. References

- [1] W. Ng, A. A. Walston, G. L. Tangonan *et al.*, "The first demonstration of an optically steered microwave phased array antenna using true-time-delay," *IEEE Journal of Lightwave Technology*, **9**, 1124-1131 (1991).
- [2] R. D. Esman, M. Y. Frankel, J. L. Dexter, *et al.*, "Fiber-optic prism true time-delay antenna feed", *IEEE Photonics Technology Letter*, **11**, 1347-1349 (1993).
- [3] L.P. Shen, W. P. Huang, G. X. Chen, *et al.*, "Design and optimization of photonic crystal fibers for broad-band dispersion compensation", *IEEE Photonics Technology Letter*, **15**, 540-542 (2003)
- [4] J.A. West, N. Venkataramam, C.M. Smith, *et al.*, "Photonic crystal fibers", *Proc. 27th Eur. Conf. on Opt. Comm. (ECOC '01)*, **4**, 582 – 585 (2001)
- [5] Y. Jiang, Z. Shi, B. Howley, R.T. Chen, "Highly Dispersive Photonic Crystal Fibers for True-Time-Delay Modules of an X-band Phased Array Antenna", *Proceedings of SPIE*, **5360**, 253-258, (2004).
- [6] K. Thyagarajan, R.K. Varshney, P. Palai, *IEEE Photonic Technology Letters*, **8**, 1510-1512 (1996)
- [7] J. Broeng, S. E. Barkou, T. Sndergaard, *et al.*, "Analysis of air-guiding photonic bandgap fibers", *Optics Letters.*, **25**, 96-98 (2000)
- [8] Z. Shi, L. Gu, B. Howley, Y. Jiang, *et al.*, "True-time-delay modules based on single tunable laser in conjunction with waveguide-hologram for phased-array antenna", *Optical Engineering*, **44**, 084301 (2005)
- [9] Y. Wipiejewski, Akulova Y.A., Schow C., "Monolithic Integration of a widely tunable laser diode with a high speed electro absorption modulator", *Electronic Components and Technology Conference 2002*, pp. 558-562 (2002)